



1 Fragmentation of DNA in a sub-microliter microfluidic sonication device†

Qingzong Tseng,^a Alexey M. Lomonosov,^b Eileen E. M. Furlong^a and Christoph A. Merten*^a

Received 23rd May 2012, Accepted 4th September 2012

DOI: 10.1039/c2lc40595d

Fragmentation of DNA is an essential step for many biological applications including the preparation of next-generation sequencing (NGS) libraries. As sequencing technologies push the limits towards single cell and single molecule resolution, it is of great interest to reduce the scale of this upstream fragmentation step. Here we describe a miniaturized DNA shearing device capable of processing sub-microliter samples based on acoustic shearing within a microfluidic chip. A strong acoustic field was generated by a Langevin-type piezo transducer and coupled into the microfluidic channel *via* the flexural lamb wave mode. Purified genomic DNA, as well as covalently cross-linked chromatin were sheared into various fragment sizes ranging from ~180 bp to 4 kb. With the use of standard PDMS soft lithography, our approach should facilitate the integration of additional microfluidic modules and ultimately allow miniaturized NGS workflows.

Introduction

Next generation sequencing (NGS) has revolutionized modern biology and is becoming an invaluable tool for diagnostics and personalized medicine.^{1,2} The time and cost to sequence 3 billion base pairs has dropped from 10 years and US\$ 3 billion for the Human Genome Project (1990–2003) to no more than 2–3 weeks and approximately US\$ 19 500 in 2011.^{3,4} In parallel, NGS tools and services have become a substantial industry with sales of about US\$ 1 billion per year.⁵ This success is partially due to the integration of microfluidic flow cells into all current NGS devices, which allowed massive miniaturization and parallelization of the sequencing reactions. On the other hand, upstream procedures such as the preparation of sequencing libraries, and in particular the fragmentation of genomic DNA into the appropriate sizes that are optimal for NGS machines (typically about 200 bp), are still carried out using macroscopic equipment and sample volumes of at least tens to hundreds of microliters. This represents a major bottleneck, especially for applications such as single cell and single molecule sequencing or analysis of patient samples.^{6,7} Hence reducing the input material is undoubtedly of major importance for further advances in the field. Although other biochemical preparation steps, such as cell sorting, cell disruption, affinity purification, electrophoresis, and PCR amplification have already been transformed into microfluidic formats,^{8,9} DNA shearing as an essential step for any NGS application remains poorly exploited in microfluidic systems.

Conventionally, DNA shearing is done either by sonication, hydrodynamic shearing, or enzymatic digestion. Even though

enzymatic digestion may be straightforward to implement in microfluidic systems, its sequence-specific cleavage and biased susceptibility for specific chromatin regions make it unsuitable for certain applications.¹⁰ Hydrodynamic shearing of DNA in microfluidic system has been reported recently, but did not allow the generation of sub-kilobase fragments essential for most NGS devices.^{11,12} This limitation could be circumvented by sonication, which is the most widely used method for bulk DNA shearing experiments including applications, such as Chromatin Immunoprecipitation (ChIP),¹³ for which small fragment sizes are absolutely crucial to obtain high resolution. The physical shearing mechanism of sonication generates DNA fragments in an unbiased fashion and is quite robust in regard to sample type and concentration.¹⁴ Therefore, the implementation of a sonication-based microfluidic shearing system would not only complement the microfluidic genomics toolbox, but might also be irreplaceable for certain applications.

Here we describe a microfluidic sonication device based on standard PDMS soft lithography. The acoustic field is generated by a composite piezoelectric transducer and coupled with the microfluidic channel *via* the flexural mode. The strong acoustic energy created inside the fluidic channel is capable of shearing both genomic DNA as well as covalently cross-linked chromatin into a wide and controllable range of fragment sizes. Its ability to process sub-microliter samples and its compatibility with other microfluidic modules make the system a desirable choice for integration into next-generation sequencing platforms as well as a stand-alone sonication device for molecular biology applications.

Results

Design of the microfluidic sonication device

The fragmentation of DNA *via* sonication is based on cavitation and mechanical degradation.¹⁵ While long DNA molecules can

^aGenome Biology Unit, European Molecular Biology Laboratory, Meyerhofstraße 1, Heidelberg, 69117, Germany.

E-mail: christoph.merten@embl.de

^bGeneral Physics Institute, Russian Academy of Sciences, 117942, Moscow, Russia

† Supplementary Information available: Experimental procedures and additional notes. See DOI: 10.1039/c2lc40595d

be sheared into smaller pieces (>10 kb) in the absence of cavitation, the generation of short fragments most likely requires free radicals produced by cavitation.^{15,16} As acoustic cavitation has been reported to be most efficient at frequencies below 100 kHz,¹⁷ we used a Langevin-type composite transducer with a fundamental resonance frequency of 63 kHz as source of the acoustic vibration. The composite transducer is made of piezo-ceramic rings clamped between two metal pieces. This configuration compensates the low-tensile strength of the ceramic, generates higher vibration amplitude and circumvents the fabrication limit of large single-piece ceramics for low ultrasonic frequencies.¹⁸ The transducer was bonded to a 1 mm-thick, 7.5 cm by 5 cm glass plate by a thermo-reversible epoxy glue (Fig. 1a).

The microfluidic sonication chamber had a diameter of 6 mm and a height of 250 μ m, and was connected to inlet/outlet channels with a width of 100 μ m. Additionally, a 400 μ m wide and 4 mm long dead end air compartment was connected perpendicular to the sonication chamber in order to increase the inclusion of

cavitation nuclei by introducing an air–liquid interface (Fig. 1a).¹⁹ The microfluidic chamber was filled by simply using a micropipette without the need for tubing and syringe pumps.

Characterization of plate oscillation

The coupling of acoustic energy through the flexural vibration mode of the glass plate has been previously exploited to generate ultrasonic fields in microfluidic channels for rapid mixing and sonochemical reactions.^{20,21} In general, this setup facilitates observations inside the microfluidic channel and avoids direct contact between the liquid sample and the transducer. For our device, bonding to a 1 mm thick glass plate, resulted in a slightly shifted resonance frequency of 74.3 kHz as determined by tracking the maximum vibration amplitude. Since the acoustic wavelength at this frequency is far longer than the thickness of the glass plate, the vibration is dominated by the lamb wave mode (see supplementary information for more details).²²

In order to determine the maximum acoustic energy coupled into the microfluidic channel, we used the probe-beam deflection

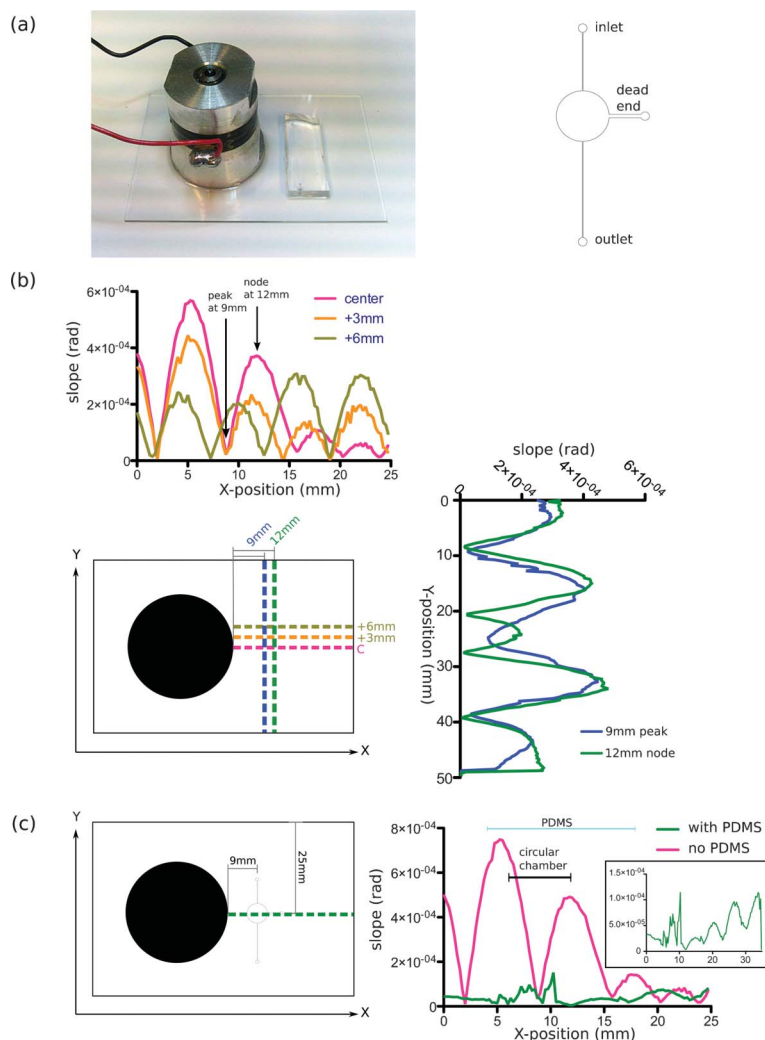


Fig. 1 Microfluidic sonication device. (a) Design of the device. A PDMS chip and a Langevin-type transducer were bonded to a glass plate (left). The geometry of the PDMS chip (right) allows sample loading using conventional micropipettes. (b) Surface profile of the glass slide at the resonance frequency (74.3 kHz) at the center, +3 mm and +6 mm along the X-axis (top) and +9 mm and +12 mm along the Y-axis (right). (c) Comparison of the vibration profile of the glass surface along the center of the Y-axis before (magenta) and after (green) bonding the PDMS chip to the slide.

(PBD) method to determine the local inclination of the plate under acoustic oscillation,²³ with the highest slope values corresponding to the nodes and lowest slope values corresponding to the peaks of the standing wave (Fig. 1b). We first scanned the glass plate along the *X*-axis to locate the maximum displacement along this axis. The deformation of the plate had a period of about 6 mm at the resonant frequency with the peak displacement located at 9 mm from the transducer (Fig. 1b top). The plate was then scanned along the shorter *Y*-axis of the plate crossing the peak and node position at 9 mm and 12 mm from the transducer. The oscillation profile followed the symmetry of the device and had a maximum on the axis of symmetry (Fig. 1b right). The local inclination measurement also allowed us to calculate the absolute value of the glass surface displacement (see supplementary information for more details), which was approximately 1.2 μm with 30 V applied to the transducer at the resonance frequency. This represents more than a 30-fold enhancement in terms of electric-acoustic conversion compared to previous devices using single piezo-ceramics as acoustic source.¹⁹

Based on the above results, the microfluidic channel was designed to have a 6 mm diameter circular sonication chamber which would cover a half period of the acoustic standing wave on the glass surface. By positioning the microfluidic chip exactly above the peak position of the acoustic oscillation, we ensured maximum displacement of the glass surface within the sonication chamber. Since the flexural lamb wave is highly sensitive to the thickness, density and elastic property of the material,²⁴ the bonding of a 5 mm thick PDMS microfluidic chip onto the glass plate might significantly alter the acoustic oscillation pattern and amplitude. For this reason, we repeated the same profile measurement on the glass surface with the microfluidic PDMS chip bonded on the back side of the glass slide. Since the lamb wave propagates symmetrically along both faces of a plate, the measurement done on the back side of the plate right under the PDMS chip is a good estimation for the real vibration amplitude within the microfluidic sonication chamber. The measurement revealed that the vibration pattern was damped and altered close to the PDMS bonded region (inset of Fig. 1c). While the resonance frequency shifted upward to 74.7 kHz after bonding the PDMS chip, the maximum amplitude reduced to 0.24 μm with 30 V applied to the transducer.

Cavitation bubble dynamics in the sonication device

The amplitude of the vibration of the glass surface generated pressure at the glass-liquid interface exceeding the cavitation threshold when higher voltage was applied to the transducer (see supplementary information). To directly observe the formation

of cavitation bubbles and their dynamics, we loaded the microfluidic sonication device with water and monitored the sonication process inside the microfluidic chamber with a high speed camera while applying 300 V to the transducer. Using a frame rate of 58 322 fps, which was about 5/4 period of the acoustic oscillation, we could clearly register the expansion and implosion of cavitation bubbles (Fig. 2 and Movie S1†). We also noticed that the initiation of the cavitation bubbles was not only limited to the air-liquid interface introduced *via* the dead-end channel. Most likely, the strong acoustic field was sufficient to generate cavitation nuclei from the dissolved gas in the liquid or from the imperfections on the PDMS channel surface.²⁵ As the formation of bubbles was observed immediately after applying electrical power and disappeared right after switching off the system, it seems unlikely that the initiation of bubbles was driven by heat.

DNA shearing in the microfluidic sonication device

To demonstrate the shearing of DNA for the preparation of NGS libraries, we next sonicated 7 μL of lambda phage genomic DNA (50 $\mu\text{g } \mu\text{L}^{-1}$) in the microfluidic chip (Fig. 3a). The resulting average fragment size could be efficiently controlled over a range from approximately 180 bp to 4 kb by either altering the applied voltage or the duration of the sonication process. This size range is not only compatible with current NGS platforms requiring \sim 200 bp fragments, but should as well be suitable for future 3rd generation sequencers, whose read length may reach 1 kb or more. Control experiments furthermore showed that the obtained peak widths was comparable to the performance of commercial bench-top sonication devices using much bigger volumes (Fig. S1†).

Shearing of chemically cross-linked chromatin is required for many assays probing DNA-protein interactions, such as Chromatin Immunoprecipitation,¹³ and Chromosome Conformation Capture.²⁶ However, due to the covalent cross-linking between protein and DNA, as well as the requirement for unbiased fragmentation, this can hardly be achieved by hydrodynamic or enzymatic shearing. As a consequence, sonication remains the most widely used protocol for the fragmentation of cross-linked chromatin.¹³ Hence we also tested the possibility to shear chromatin in the microfluidic device. In particular, we sonicated 500 ng of cross-linked chromatin from *Drosophila melanogaster* embryos (in a total volume of 7 μL nuclear lysis buffer) on-chip, followed by reverse-crosslinking, purification and analysis by agarose gel electrophoresis (Fig. 3b). After 10 min of sonication, the majority of the fragments showed an average size of approximately 197 bp and 353 bp when applying a voltage of 250 V and 200 V, respectively. The integrity of the sheared



Fig. 2 Cavitation bubble dynamics. Snapshots of bubbles expanding (at 0, 34.3, 68.6, and 120.05 μs) and imploding (17.15, 51.45, and 85.75 μs) were obtained using a high speed camera operating at 58,322 fps. An AC signal of 300 V and 74.3 kHz was applied to the Langevin-type transducer and images were taken at the indicated time points. Scale bar = 50 μm .

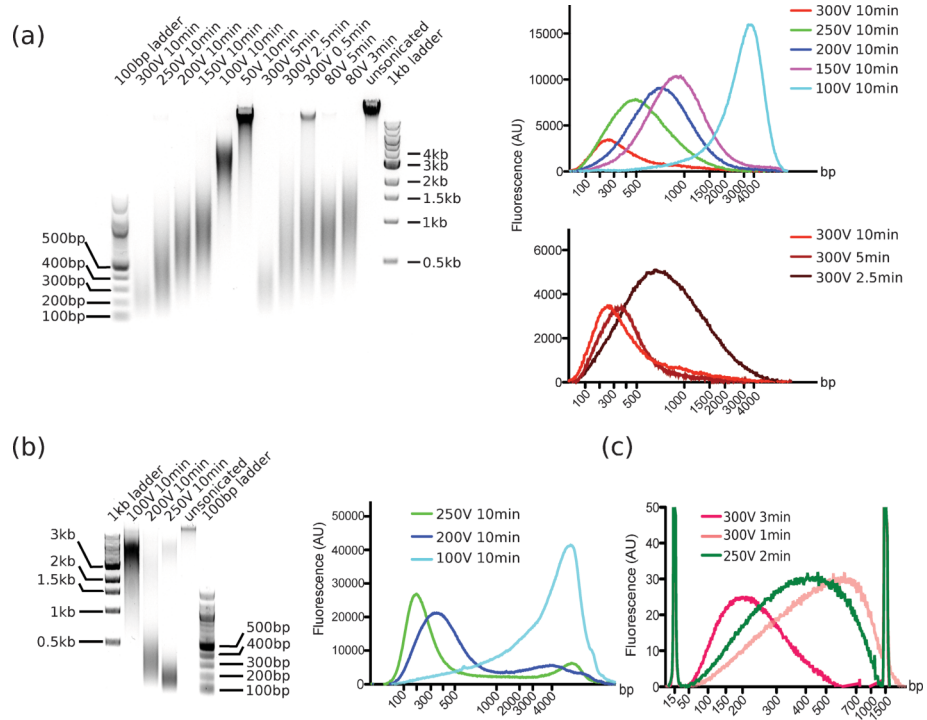


Fig. 3 Fragmentation of DNA in the microfluidic sonication device. (a) Agarose gel image and fluorescent line scan of the fragmentation products after sonication of $7 \mu\text{l}$ ($50 \text{ ng } \mu\text{l}^{-1}$) of 48 kb λ -phage genomic DNA at different voltages and pulse durations. (b) Agarose gel image and fluorescent line scan of the fragmentation products after sonication of $7 \mu\text{l}$ (500 ng) cross-linked chromatin from *Drosophila melanogaster* embryos. (c) Electrogram of the fragmentation products after sonication of $0.7 \mu\text{l}$ ($50 \text{ ng } \mu\text{l}^{-1}$) λ phage DNA, as obtained using an Agilent 2100 Bioanalyzer DNA1000 chip. Different voltages and pulse durations are indicated by different colors.

chromatin was verified by immunoblotting using antibodies against RNA polymerase II (Pol II), hence clearly demonstrating that the protein epitopes were preserved during the sonication procedure (Fig. S2†).

Unlike hydrodynamic shearing which depends strongly on the flow rate, sonication based shearing can be more easily scaled down to very small sample amounts, as long as the acoustic energy is efficiently delivered into the microfluidic channel. To validate this capability, a shallower reservoir with a depth of $20 \mu\text{m}$ and the same diameter was used to sonicate $0.7 \mu\text{L}$ of lambda phage DNA. The sonicated samples were subsequently diluted 2-fold and analyzed by using an Agilent 2100 Bioanalyzer DNA1000 chip (Fig. 3c). Fragments centered at 195 bp, 436 bp and 583 bp were generated from given sonication conditions (300 V for 3 min , 250 V for 2 min , and 300 V for 1 min), which confirmed the ability of processing sub-microliter sample volumes.

Conclusions

We present here a simple and low cost microfluidic sonication setup. Our system could shear both, naked DNA and crosslinked chromatin into various fragment sizes in a controlled manner similar to conventional bench-top sonicators. In addition, its ability to generate smaller fragments and to process sub-microliter sample volumes has not been demonstrated previously. In theory, the minimum sample size could be decreased further by using a smaller diameter of the sonication chamber or simply by using nanoliter volume channels (with small cross sections) instead of a relatively large circular reservoir. By

directly attaching a commercially available Langevin-type transducer ($\sim \text{US\$ 20}$) to a standard microscopic slide, we generated a high intensity acoustic field within a standard PDMS microfluidic chip *via* flexural vibration of the plate. This configuration is highly flexible, allows microscopic observations of the sample and should facilitate the integration of additional microfluidic modules into the system. Furthermore, the use of a Langevin-type transducer made the electric-acoustic conversion approximately 30-fold more efficient compared to single piezoceramic transducers. This capability to generate strong acoustic power also opens up other on-chip applications such as cell lysis, homogenization of tissue and direct extraction of genomic material.²⁷ Considering the additional cost of a low power ultrasonic generator ($<\text{US\$ 1000}$), the whole setup represents a competitive sonication device for small volumes. The low cost of the PDMS chip itself ($<\text{US\$ 3}$; the transducer can be recycled) even allows for single-run experiments to completely rule out any cross-contamination during the preparation of NGS sequencing libraries. We believe that the capability to process sub-microliter volume, and the simple configuration which facilitates future integration into other microfluidic designs, will pave the way for genomic analysis toward single-cell and single-molecule levels.

Experimental procedures

Biological sample preparation

Lambda phage DNA (D9768, Sigma) was dissolved in water to a final concentration of $50 \text{ ng } \mu\text{L}^{-1}$ before use. Formaldehyde

crosslinked chromatin from *Drosophila melanogaster* embryos was prepared as previously described.¹ Approximately 500 ng of chromatin dissolved in 7 μ L of nuclear lysis buffer (50 mM HEPES, pH 8, 10 mM EDTA-Na₂, 0.5% N-Lauroylsarcosine) was loaded on chip for sonication. Sonicated phage DNA was analyzed directly on an EtBr stained 1% agarose gel, while chromatin was first diluted with water to 100 μ L containing 0.5% SDS and 0.5 mg mL⁻¹ proteinase K, and then incubated at 65 °C for 3 h. De-crosslinked chromatin was subsequently purified using a QIAquick spin column (28104, Qiagen) and finally eluted in 30 μ L water. 5 μ L of the purified chromatin was analyzed on a 1% agarose gel.

For sonication of 0.7 μ L of phage DNA, sonicated samples were first diluted 2-fold before 1 μ L was analyzed using an Agilent 2100 Bioanalyzer DNA1000 chip.

Fabrication of the microfluidic device

SU8-2150 or SU8-2050 photoresists (Microchem) were spin coated on 3-inch silicon wafers (Silicon Materials, Germany) at speeds corresponding to a resulting layer thickness of 250 μ m and 20 μ m, respectively. Following a standard lithography protocol given by the supplier, the photoresist was soft baked for 5 min at 90 °C, before the channel patterns (printed as mirrored negatives on a CAD-designed 25,400 dpi high resolution photomask; Selba, Switzerland) were projected onto the wafer using 365 nm UV light (MA-45 Mask Aligner, Süss Microtec, Germany). After exposure for 40 s (10 s for 20 μ m thick resist), the wafer was again baked for 5 min at 90 °C. Development was done by incubating the wafer three consecutive times in MR-Dev-600 (Microchem) with occasional agitation. Finally, the wafer was hard baked at 150 °C for 3 min.

After development, the resulting silicon master mold was filled with 5 mm thick 1 : 10 (curing agent:base) PDMS (Sylgard 184, Dow Corning) and cured at 65 °C for 16 h. Cured PDMS chips were cut and peeled off from the mold before inlet and outlet connections were punched using a 0.75 mm biopsy punch (Unicore, Harris). Subsequent to treatment in an oxygen plasma oven (FEMTO, Diener Electronics) at 25 W for 90 s, the chip was closed by bonding to a 1 mm thick 75 mm \times 50 mm glass slide (PLANO, Germany).

In a second step, the Langevin-type transducer (MPI-2525D-60H, UltrasonicWorld) was mounted to the glass slide at approximately 10 mm from the three closest edges using two-component epoxy glue (Endfast300, UHU) cured at 120 °C. Electric wires were welded to the copper electrodes of the transducer using standard tin solder.

Operation of the microfluidic sonication device

A function generator (148A, Wavetek) was used to generate a sinusoidal signal which was amplified by a high voltage amplifier (623B, TREK). The amplified AC signal was then sent to the transducer. The resulting working voltage and current were monitored through a build-in monitor port on the amplifier via a digital oscilloscope (PM3394A, Philips). For sonication experiments, the whole device was supported at four corners by 6 mm \times 6 mm \times 3 mm ($L \times W \times H$) PDMS (1 : 10) cubes. The AC signal was also amplitude modulated for 5 s ON and 5 s OFF. For microscopic observation, the device was mounted on a

custom made slide holder supporting only the outermost 5 mm of the four edges. A high speed camera (EoSens mini1, Mikrotron) was attached to the side port of an inverted microscope (Eclipse Ti, Nikon). The image capture was done using MotionBLITZ Director software at a rate of 58 322 fps.

Sample analysis

Agarose gel images were taken on a gel documentation system (Quantum, peqlab), then analyzed by ImageJ (<http://rsb.info.nih.gov/ij/>) using the plot profile function for each electrophoresis lane. The size of the major peaks was determined by generating a calibration curve (size *vs.* migration distance) using 100 bp and 1 kb DNA ladders (N3231/N3232, NEB) and interpolating it for the observed migration distances.

The data from the Bioanalyzer were retrieved as raw data (fluorescent intensities *vs.* migration time). Curves were first baseline corrected, and then normalized to the 1500 bp marker peak. The size increments indicated on the *X*-axis (Fig. 3) were directly mapped using the ladder without interpolation.

Measurement of the plate vibration

Oscillations of the plate were measured by means of the noncontact laser probe-beam deflection (PBD) technique. A cw laser beam (Compass 315M-150, Coherent) with a wavelength of 533 nm was focused sharply onto the glass plate. The reflected beam was fed into a custom-made differential position-sensitive detector made from two juxtaposed photodiodes and a preamplifier, which generated a signal proportional to the local inclination of the plate. The PBD setup was calibrated using a custom-made rotating reflector. The ultrasonic transducer was tuned to the main resonance of the plate at 74.3 kHz. Distribution of the slope amplitude has been measured by scanning the plate along given axes with a step size of 250 μ m.

Western blot analysis

5 μ L of sheared chromatin (~350 ng) were subjected to electrophoresis in 4-12% gradient SDS/PAGE gels (NuPAGE, Invitrogen) at 90 V for 3 h, and transferred to a PVDF membrane at 30 V at 4 °C for 16 h. The membrane was then blocked and immunostained firstly by mouse anti-Pol II antibody (ab5408, Abcam) and then by HRP conjugated Donkey anti-mouse IgG secondary antibody (Jackson ImmunoResearch). The immunoblot was finally visualized by using a chemiluminescence kit (Western Lightening ECL, PerkinElmer).

Acknowledgements

We would like to thank Peter Hess and Yad Ghavi-Helm for kindly providing experimental equipment and materials.

References

- 1 M. L. Metzker, *Nat. Rev. Genet.*, 2009, **11**, 31–46.
- 2 D. Eicher and C. A. Merten, *Expert Rev. Mol. Diagn.*, 2011, **11**, 505–519.
- 3 F. S. Collins, M. Morgan and A. Patrinos, *Science*, 2003, **300**, 286–290.
- 4 E. S. Lander, *Nature*, 2011, **470**, 187–197.
- 5 A. Coombs, *Nat. Biotechnol.*, 2008, **26**, 1109–1112.

6 E. E. Schadt, S. Turner and A. Kasarskis, *Hum. Mol. Genet.*, 2010, **19**, R227–R240.

7 J. F. Thompson and P. M. Milos, *Genome Biol.*, 2011, **12**, 217.

8 S. Vyawahare, A. D. Griffiths and C. A. Merten, *Chem. Biol.*, 2010, **9**, R. N. Zare and S. Kim, *Annu. Rev. Biomed. Eng.*, 2010, **12**, 187–201.

10 M. Flavin, L. Cappabianca, C. Kress, H. Thomassin and T. Grange, *Mol. Cell. Biol.*, 2004, **24**, 7891–7901.

11 L. Shui, J. G. Bomer, M. Jin, E. T. Carlen and A. van den Berg, *Nanotechnology*, 2011, **22**, 494013.

12 I. V. Nesterova, M. L. Hupert, M. A. Witek and S. A. Soper, *Lab Chip*, 2012, **12**, 1044–1047.

13 P. J. Park, *Nat. Rev. Genet.*, 2009, **10**, 669–680.

14 A. T. Bankier, *Methods Mol. Biol.*, 1993, **23**, 47–50.

15 H. I. Elsner and E. B. Lindblad, *DNA*, 1989, **8**, 697–701.

16 H. Galperin-Lemaitre, M. Kirsch-Volders and S. Levi, *Hum. Genet.*, 1975, **29**, 61–66.

17 J. P. Lorimer and T. J. Mason, *Chem. Soc. Rev.*, 1987, **16**, 239.

18 J. A. Gallego Juárez, *Rev. Acust.*, 2002, **33**, 36–42.

19 Tandiono, S.-W. Ohl, D. S.-W. Ow, E. Klaseboer, V. V. T. Wong, A. Camattari and C.-D. Ohl, *Lab Chip*, 2010, **10**, 1848–1855.

20 Tandiono, S.-W. Ohl, D. S. W. Ow, E. Klaseboer, V. V. Wong, R. Dumke and C.-D. Ohl, *Proc. Natl. Acad. Sci. U. S. A.*, 2011, **108**, 5996–5998.

21 D. Ahmed, X. Mao, J. Shi, B. K. Juluri and T. J. Huang, *Lab Chip*, 2009, **9**, 2738–2741.

22 R. W. B. Stephens and A. E. Bate, *Acoustics and vibrational physics*, 1966.

23 A. Lomonosov, V. G. Mikhalevich, P. Hess, E. Y. Knight, M. F. Hamilton and E. A. Zabolotskaya, *J. Acoust. Soc. Am.*, 1999, **105**, 2093–2096.

24 S. S. Kessler, S. M. Spearing and C. Soutis, *Smart Mater. Struct.*, 2002, **11**, 269–278.

25 C. E. Brennen, *Cavitation and Bubble Dynamics*, Oxford University Press, 1995.

26 M. J. Fullwood and Y. Ruan, *J. Cell. Biochem.*, 2009, **107**, 30–39.

27 D. Chen, *Handbook on Applications of Ultrasound: Sonochemistry for Sustainability*, CRC Press, 2011.